Numerical Study of Chemically Reacting Flows Using a Lower-Upper Symmetric Successive Overrelaxation Scheme

Jian Shun Shuen*
NASA Lewis Research Center, Cleveland, Ohio
and
Seokkwan Yoon†
NASA Ames Research Center, Moffett Field, California

A new computational fluid dynamics code has been developed for the study of mixing and chemical reactions in the flowfields of ramjets and scramjets. The code employs an implicit finite-volume, lower-upper symmetric successive overrelaxation (LU-SSOR) scheme for solving the complete two-dimensional Navier-Stokes equations and species transport equations in a fully coupled and very efficient manner. The combustion processes are modeled by an 8-species, 14-step, finite-rate chemistry model, and the turbulence is simulated by a Baldwin-Lomax algebraic model. The validity of the code is demonstrated by comparing the numerical calculations with both experimental data and previous calculations of a cold-flow helium injection into a straight channel and premixed hydrogen-air reacting flow in a ramped duct. The code is then used to calculate the mixing and chemical reactions of a hydrogen jet transversely injected into a supersonic airstream. Results are presented that describe the flowfield, the recirculation regions in front of and behind the injector, and the chemical reactions.

Nomenclature

C_{p_i} = constant-pressure specific heat of species i
C_{v_i} = constant-volume specific heat of species i
D_{ij} = binary diffusion coefficient
e = total internal energy
h_i = enthalpy of species i
h_{fi}° = heat of formulation of species i
I = identity matrix
M_i = molecular weight of species i
N_s = number of species
Pr_t = turbulent Prandtl number
p = pressure
q = heat flux
R_u = universal gas constant
Sc_t = turbulent Schmidt number
T = temperature
t = time
u = streamwise velocity
$\tilde{u}_i$ = streamwise diffusion velocity of species i
v = transverse velocity
$\tilde{v}_i$ = transverse diffusion velocity of species i
X_i = molar fraction of species i
x,y,z = Cartesian coordinates
Y_i = mass fraction of species i
μ = viscosity
ρ = density
τ = stress tensor

Subscripts and Superscripts

i,j = x and y grid indices, respectively
n = time index

Presented as Paper 88-0436 at the AIAA Aerospace Sciences Meeting, Reno, NV, Jan 11-14, 1988; received March 21, 1988; revision received Aug. 6, 1988.

*Senior Research Engineer, Sverdrup Technology, Inc., NASA Lewis Research Center Group. Member AIAA.
†Senior Research Engineer, MCAT Institute. Member AIAA.

Introduction

THE recent interest in hypersonic vehicles has created a need for efficient numerical methods to predict turbulent mixing and combustion in transonic and supersonic flows. In the development of such predictive methods, numerical stability and efficiency have to be considered. The stability problem arises mainly from the stiffness of the chemical source terms in the species concentration equations, whereas the need for numerical efficiency results from the large number of species equations that have to be solved along with the flow equations and the close coupling between flow and chemistry. In recent years, a number of numerical methods[1-4] have been developed to calculate steady-state supersonic reacting flows. Most of these methods have treated chemical source terms implicitly to remove the stiffness associated with the species equations. Although this approach has been successful in circumventing the stiffness limitation, most existing methods have suffered from numerical inefficiency. The majority of the reacting flow codes developed to date have adopted explicit integration methods in which the flow and the species equations are solved sequentially and are not directly coupled. Because in most chemically reacting flows, the coupling between species and flow variables is strong, explicit methods are generally not robust and converge very slowly. Most implicit methods, such as the popular Beam and Warming scheme,[5] on the other hand, require the inversion of large block banded matrices, which can be very costly when a large number of species equations are solved in a coupled manner with the flow equations.

In the present paper, a new numerical method is described for the study of mixing and chemical reactions in transonic and supersonic flows. It employs an implicit finite-volume, lower-upper symmetric overrelaxation (LU-SSOR) scheme for solving the complete two-dimensional Navier-Stokes equations and species transport equations in a fully coupled manner, with real gas properties. This scheme treats the inviscid flux and chemical source terms implicitly but treats viscous term explicitly. Despite being implicit, the LU scheme requires only scalar diagonal inversions for nonreacting flows and block-diagonal inversion for reacting flows, which saves considerable CPU time without using a diagonalization procedure. Furthermore, because of the special structure of the left-hand-side (LHS) LU operators in the LU-SSOR scheme, the two L and U operators can be fully vectorized, whereas the

LHS operators in most other implicit schemes are not vectorizable. The second author[6,7] has recently developed the LU-SSOR scheme for nonreacting flows, and extensive tests have shown that this scheme is very robust and efficient for transonic and supersonic nonreacting flows. The objective of the present paper is then to demonstrate the efficiency of the new LU-SSOR scheme in calculating chemically reacting flows.

Several mixing and/or combustion problems are considered in this study. They include a cold-flow helium injection, premixed hydrogen and air reacting flows in a ramped duct, and a transverse injection of hydrogen into a supersonic airstream with combustion. The chemical reactions are represented by an 8-species, 14-step chemistry model of Westbrook[8] and Hitch et al.[9] The governing equations are Reynolds-averaged, and the closure of the equations is provided by the algebraic eddy viscosity model of Baldwin and Lomax.[10]

Analysis

Governing Equations

The two-dimensional unsteady Navier-Stokes and species transport equations for chemically reacting flows, in Cartesian coordinates, are given by[11,12]

$$\frac{\partial Q}{\partial t} + \frac{\partial (F - F_v)}{\partial x} + \frac{\partial (G - G_v)}{\partial y} = S \tag{1}$$

where

$$Q = \begin{bmatrix} \rho \\ \rho u \\ \rho v \\ \rho e \\ \rho_{Yi} \end{bmatrix} \quad F = \begin{bmatrix} \rho u \\ \rho u^2 + p \\ \rho uv \\ u(\rho e + p) \\ \rho u_{Yi} \end{bmatrix} \quad G = \begin{bmatrix} \rho v \\ \rho uv \\ \rho v^2 + p \\ v(\rho e + p) \\ \rho v_{Yi} \end{bmatrix}$$

$$F_v = \begin{bmatrix} 0 \\ \tau_{xx} \\ \tau_{xy} \\ u\tau_{xx} + v\tau_{xy} - q_x \\ -\rho \tilde{u}_{iY_i} \end{bmatrix} \quad G_v = \begin{bmatrix} 0 \\ \tau_{xy} \\ \tau_{yy} \\ u\tau_{xy} + v\tau_{yy} - q_y \\ -\rho \tilde{v}_{iY_i} \end{bmatrix}$$

$$S = \begin{bmatrix} 0 \\ 0 \\ 0 \\ 0 \\ \dot{W}_i \end{bmatrix}, \qquad i = 1,2, \ldots, N_s - 1$$

and

$$\tau_{xx} = 2\mu u_x - \tfrac{2}{3}\mu(u_x + v_y)$$

$$\tau_{xy} = \mu(u_y + v_x)$$

$$\tau_{yy} = 2\mu v_y - \tfrac{2}{3}\mu(u_x + v_y)$$

$$q_x = -k\frac{\partial T}{\partial x} + \rho \sum_{i=1}^{N_s} h_i Y_i \tilde{u}_i$$

$$q_y = -k\frac{\partial T}{\partial y} + \rho \sum_{i=1}^{N_s} h_i Y_i \tilde{v}_i$$

The diffusion velocities are found by Fick's law,

$$Y_i\tilde{u}_i = -D_i \frac{\partial}{\partial x} Y_i, \qquad Y_i\tilde{v}_i = -D_i \frac{\partial}{\partial y} Y_i \tag{2}$$

and

$$\mu = \mu_{\text{laminar}} + \mu_{\text{turbulent}}$$

$$k = k_{\text{laminar}} + k_{\text{turbulent}}$$

$$D_i = D_{i_{\text{laminar}}} + D_{i_{\text{turbulent}}}$$

where $D_{i_{\text{laminar}}} = (1 - X_i)/\sum_{j \neq i}(X_i/D_{ij})$ is the laminar binary diffusivity of species i in the gas mixture.[12] The temperature and pressure are calculated iteratively from the following equations:

$$e = \sum_{i=1}^{N_s} Y_i h_i - \frac{p}{\rho} + \frac{1}{2}(u^2 + v^2) \tag{3}$$

$$h_i = h_{fi}^{\circ} + \int_{T_{\text{Ref}}}^{T} C_{p_i} dT \tag{4}$$

$$p = \rho R_u T \sum_{i=1}^{N_s} \frac{Y_i}{M_i} \tag{5}$$

Thermodynamics and Transport Models

The specific heat, thermal conductivity, and viscosity for each species are determined by fourth-order polynomials of temperature. The coefficients of these polynomials are supplied by McBride[13] and are valid up to a temperature of 6000 K. The specific heat of the gas mixture is obtained by mass concentration weighting of each species. The thermal conductivity and viscosity of the mixture, however, are calculated using Wilke's mixing rule.[14]

The binary mass diffusivity D_{ij} between species i and j is obtained using the Chapman-Enskog theory in conjunction with the Lennard-Jones intermolecular potential functions.[14] The diffusion of a species in the gas mixture is approximated by Fick's law (i.e., treating the species i and the surrounding gas as a binary gas mixture), and the diffusion velocities for each species are calculated using Eq. (2). It should be noted that Fick's law is a convenient approximation of the multicomponent diffusion equations obtained from the kinetic theory of gases, and the error introduced by the approximation may become significant if the pressure gradients in the flowfield are very large or the molecular weights of the species are very different.[12]

Chemistry and Turbulence Models

In the present study, an 8-species, 14-step chemistry model is adopted for hydrogen-air reactions. This model is a reduced H_2-air reaction scheme developed from a sensitivity analysis by Hitch et al.[9] performed on a more complete model originally proposed by Westbrook.[8] This reduced reaction mechanism was shown to yield good agreement with the more complete model for both the ignition delay and the reaction times over a wide range of conditions.[9] It was also shown in Ref. 9 that the 2-step global model developed by Rogers and Chinitz[15] predicted much shorter ignition times and longer reaction times compared to the 14-step model used in the present study.

The closure of the governing equations is provided by the Baldwin-Lomax (B-L)[10] algebraic eddy viscosity model and constant turbulent Prandtl and Schmidt numbers ($Pr_t = Sc_t = 0.9$). This model is chosen for its simplicity and computational efficiency.

Because of the nonlinear nature of chemical kinetics, effects of turbulence on reaction rates can be large, especially in regions with high turbulence intensity, such as the mixing layer, the recirculation zone, and the region near the fuel injector. To account for such interaction effects would require a very sophisticated turbulence reaction closure or a direct numerical simulation (DNS). Because no effective turbulent combustion model with finite-rate chemistry is currently avail-

able and the DNS methods for complex reacting flows are still under development, the interactions between turbulence and chemistry are not considered in the present study.

Numerical Method

LU-SSOR Scheme

Various numerical techniques have been used to solve the set of equations governing chemically reacting flows. Among these techniques, explicit schemes are generally slow to converge when the flow involves high rates of chemical reactions and heat release or large zones of recirculation. Most implicit schemes, on the other hand, require the inversion of banded block matrices and become exceedingly expensive when the chemical system involves a large number of species. In the present study, the lower-upper symmetric successive overrelation (LU-SSOR) scheme of Yoon and Jameson[6,7] is adopted to solve the coupled two-dimensional Navier-Stokes and species transport equations. The LU-SSOR scheme employs an implicit Newton iteration technique to solve the finite-volume approximation of the steady-state version of the governing equations. In this scheme, the convective flux and chemical source terms are treated implicity, whereas the viscous terms are treated explicity. Although the system of equations is formulated in a fully coupled manner, the LU-SSOR scheme requires only scalar diagonal inversion for the flow equations and diagonal block inversion for the species equations, whereas most other implicit schemes require the inversion of block banded (tridiagonal or pentadiagonal) matrices for the entire equation set. As a result, the LU-SSOR scheme has the advantage of a fast convergence rate while requiring an operational count similar to that of an explicit scheme and therefore is particularly attractive for reacting flows with large chemical systems. The convergence of the Newton integration method is assured by the diagonal dominance of the coefficient matrices of the LU-SSOR scheme.

In the following, for simplicity, the derivation of the LU-SSOR scheme will be presented for the Euler equations. The final formulation for the Navier-Stokes equations will be given at the end of the derivation. A prototype implicit scheme for a system of nonlinear hyperbolic equations such as the Euler equations can be formulated as

$$Q^{n+1} = Q^n - \beta\Delta t\{D_xF(Q^{n+1}) + D_yG(Q^{n+1}) - S^{n+1}\} - (1-\beta)\Delta t\{D_xF(Q^n) + D_yG(Q^n) - S^n\} \tag{6}$$

where D_x and D_y are difference operators that approximate $\partial/\partial x$ and $\partial/\partial y$, and β is a positive number between 0 and 1. Here n denotes the time level. In this form, the scheme is too expensive since it calls for the solution of coupled nonlinear equations at each time step. Let the Jacobian matrices be

$$A = \frac{\partial F}{\partial Q}, \qquad B = \frac{\partial G}{\partial Q}, \qquad H = \frac{\partial S}{\partial Q} \tag{7}$$

and the correction be

$$\delta Q = Q^{n+1} - Q^n$$

The scheme can be linearized by setting

$$F(Q^{n+1}) = F(Q^n) + A\,\delta Q + 0(\|\delta Q\|^2)$$

$$G(Q^{n+1}) = G(Q^n) + B\,\delta Q + 0(\|\delta Q\|^2)$$

$$S(Q^{n+1}) = S(Q^n) + H\,\delta Q + 0(\|\delta Q\|^2)$$

and dropping terms of the second and higher order. This yields

$$\{I + \beta\Delta t(D_xA + D_yB - H)\}\delta Q + \Delta tR = 0 \tag{8}$$

where R is the residual,

$$R = D_xF(Q^n) + D_yG(Q^n) - S^n$$

If $\beta = \frac{1}{2}$, the scheme remains second order time accurate while the time accuracy drops to first order for other values of β.

The unfactored implicit scheme [Eq. (8)] produces a large block banded matrix that is very costly to invert and requires large amounts of storage. Most researchers have adopted the ADI scheme, which replaces the operator of Eq. (8) by the product of two one-dimensional operators,

$$LxLy\,\delta Q = -\Delta tR \tag{9}$$

This scheme requires relatively expensive tridiagonal or pentadiagonal block matrix inversions. Linear stability analysis has shown that the ADI scheme is unconditionally stable for two-dimensional flows. In the three-dimensional case, however, the ADI scheme is unconditionally unstable. Although artificial dissipation has a stabilizing effect, a large amount of dissipation can impair the accuracy.

Yoon and Jameson[6,7] developed a lower-upper (LU) factored implicit scheme that is unconditionally stable in any number of space dimensions. We begin with a diagonally dominant form of Eq. (8),

$$\{I + \beta\Delta t(D_x^-A^+ + D_x^+A^- + D_y^-B^+ + D_y^+B^- - H)\}\delta Q = -\Delta tR \tag{10}$$

where D_x^- and D_y^- are backward-difference operators and D_x^+ and D_y^+ are forward-difference operators. Here, two-point operators are used for steady flow calculations. A^+, A^-, B^+, and B^- are constructed so that the eigenvalues of $(+)$ matrices are non-negative and those of $(-)$ matrices are nonpositive. The development of these matrices is important for the success of LU-type schemes. One possibility, which has yielded good results in the past[6,7,16] and which is used in this work, is

$$A^+ = \tfrac{1}{2}(A + \nu_AI), \qquad A^- = \tfrac{1}{2}(A - \nu_AI)$$

$$B^+ = \tfrac{1}{2}(B + \nu_BI), \qquad B^- = \tfrac{1}{2}(B - \nu_BI) \tag{11}$$

where

$$\nu_A \geq \max(|\lambda_A|), \qquad \nu_B \geq \max(|\lambda_B|) \tag{12}$$

Here, λ_A and λ_B represent eigenvalues of Jacobian matrices. After manipulation, Eq. (10) can be written as

$$\left\{\left[I + \beta\Delta t\left(\frac{A^+}{\Delta x} - \frac{A^-}{\Delta x}\right) + \left(\frac{B^+}{\Delta y} - \frac{B^-}{\Delta y}\right)\right] + \beta\Delta t\left[D_x^-A^+ + D_x^+A^- + D_y^-B^+ + D_y^+B^- - \left(\frac{A^+}{\Delta x} - \frac{A^-}{\Delta x}\right) - \left(\frac{B^+}{\Delta y} - \frac{B^-}{\Delta y}\right) - H\right]\right\}\delta Q = -\Delta tR \tag{13}$$

If we take $(+)$ and $(-)$ matrices as given in Eq. (11), then,

$$A^+ - A^- = \nu_AI$$

$$B^+ - B^- = \nu_BI \tag{14}$$

Equation (13) can then be factorized to the following form

$$\left\{C + \left[\beta\Delta t\left(D_x^- A^+ + D_y^- B^+ - \frac{A^+}{\Delta x} - \frac{B^+}{\Delta y} - H\right)\right]\right\} C^{-1} \times \left\{C + \left[\beta\Delta t\left(D_x^+ A^- + D_y^+ B^- + \frac{A^-}{\Delta x} + \frac{B^-}{\Delta y}\right)\right]\right\}\delta Q = -\Delta t R \tag{15}$$

where

$$C = I + \beta\Delta t\left[\left(\frac{A^+}{\Delta x} - \frac{A^-}{\Delta x}\right) + \left(\frac{B^+}{\Delta y} - \frac{B^-}{\Delta y}\right)\right] = \left\{1 + \beta\Delta t\left(\frac{\nu_A}{\Delta x} + \frac{\nu_B}{\Delta y}\right)\right\} I$$

If $\beta = 1$, the scheme reduces to a Newton iteration in the limit $\Delta t \to \infty$,

$$\left(D_x^- A^+ + D_y^- B^+ - \frac{A^-}{\Delta x} - \frac{B^-}{\Delta x} - H\right)\left[\left(\frac{\nu_A}{\Delta x} + \frac{\nu_B}{\Delta y}\right) I\right]^{-1} \times \left(D_x^+ A^- + D_y^+ B^- + \frac{A^+}{\Delta x} + \frac{B^+}{\Delta y}\right)\delta Q = -R \tag{16}$$

which may be written as

$$\left(D_x^- A^+ + D_y^- B^+ - \frac{A^-}{\Delta x} - \frac{B^-}{\Delta y} - H\right) \times \left(D_x^+ A^- + D_y^+ B^- + \frac{A^+}{\Delta x} + \frac{B^+}{\Delta y}\right)\delta Q = -\left(\frac{\nu_A}{\Delta x} + \frac{\nu_B}{\Delta y}\right)(D_x F + D_y G - S) \tag{17a}$$

This equation implies [see Eq. (14)]

$$\left[\left(\frac{\nu_A}{\Delta y} + \frac{\nu_B}{\Delta y}\right) I - \frac{A^+_{i-1,j}}{\Delta x} - \frac{B^+_{i,j-1}}{\Delta y} - H\right] \times \left[\left(\frac{\nu_A}{\Delta x} + \frac{\nu_B}{\Delta y}\right) I + \frac{A^-_{i+1,j}}{\Delta x} + \frac{B^-_{i,j+1}}{\Delta y}\right]\delta Q = -\left(\frac{\nu_A}{\Delta x} + \frac{\nu_B}{\Delta y}\right)(D_x F + D_y G - S) \tag{17b}$$

for the Navier-Stokes equations, F and G on the right-hand side of Eq. (17b) are replaced by $F - F_v$ and $G - G_v$. That is,

$$\left[\left(\frac{\nu_A}{\Delta x} + \frac{\nu_B}{\Delta y}\right) I - \frac{A^+_{i-1,j}}{\Delta x} - \frac{B^+_{i,j-1}}{\Delta y} - H\right] \times \left[\left(\frac{\nu_A}{\Delta x} + \frac{\nu_B}{\Delta y}\right) I + \frac{A^-_{i+1,j}}{\Delta x} + \frac{B^-_{i,j+1}}{\Delta y}\right]\delta Q = -\left(\frac{\nu_A}{\Delta x} + \frac{\nu_B}{\Delta y}\right)[D_x(F - F_v) + D_y(G - G_v) - S] \tag{18}$$

Flux and Source Jacobians

The development of flux Jacobians A and B requires the evaluation of derivatives of pressure with respect to other independent variables. The exact formulation of these derivatives is quite complicated for flows involving real gases with nonequilibrium chemistry.[17] An alternative that yields a much simpler formulation uses the concept of "equivalent gamma." Let

$$\bar{\gamma} = h_{s_m}/e_{s_m} = \left(\sum_{i=1}^{N_s} Y_i \int_0^T C_{p_i} dt\right) \Big/ \left(\sum_{i=1}^{N_s} Y_i \int_0^T C_{v_i} dt\right) \tag{19}$$

Here $\bar{\gamma}$ denotes the equivalent γ, and h_{s_m} and e_{s_m} are the sensible enthalpy and internal energy (excluding the kinetic energy and heat of formation) for the gas mixture. With the help of Eq. (19), the relationship for pressure can be written as

$$p = (\bar{\gamma} - 1)\rho e_{s_m} = (\bar{\gamma} - 1)\left[\rho e - \rho h^\circ_{f_m} - \frac{\rho}{2}(u^2 + v^2)\right] \tag{20}$$

where $h^\circ_{f_m}$ is the heat of formation of the gas mixture,

$$h^\circ_{f_m} = \sum_{i=1}^{N_s} Y_i h^\circ_{f_i}$$

Since only $N_s - 1$ species equations are actually solved, Eq. (20) needs to be rearranged to the following forms:

$$P = (\bar{\gamma} - 1)\left[\rho e - \sum_{i=1}^{N_s - 1} \rho Y_i h^\circ_{f_i} - \left(\rho - \sum_{i=1}^{N_s - 1} \rho Y_i\right) h^\circ_{f_{N_s}} - \frac{\rho}{2}(u^2 - v^2)\right] = (\bar{\gamma} - 1)\left[\rho e - \rho h^\circ_{f_{N_s}} - \sum_{i=1}^{N_s - 1} \rho Y_i \Delta h^\circ_{f_i} - \frac{\rho}{2}(u^2 - v^2)\right] \tag{21}$$

where

$$\Delta h^\circ_{f_i} = h^\circ_{f_i} - h^\circ_{f_{N_s}}$$

for real gases it is obvious that $\bar{\gamma} = \bar{\gamma}(e, \rho, \gamma_i)$. However, as discussed by Golella and Glaz,[18] this function of $\bar{\gamma}$ varies very slowly with the change of other thermodynamic and flow properties; thus, we have treated $\bar{\gamma}$ as a local constant in the evaluation of pressure derivatives. This approximation will not affect the accuracy of the converged steady-state solution.

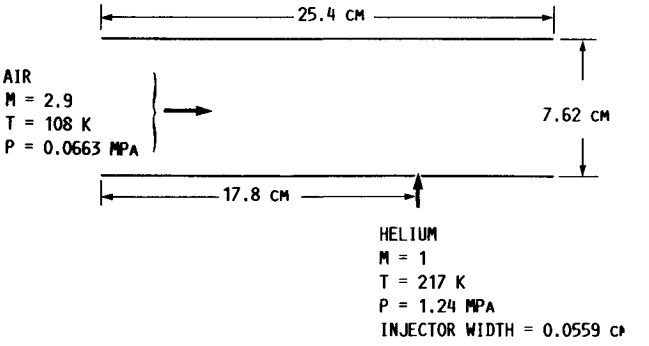

Fig. 1 Geometry and inflow conditions for the mixing of air and a transverse He jet.

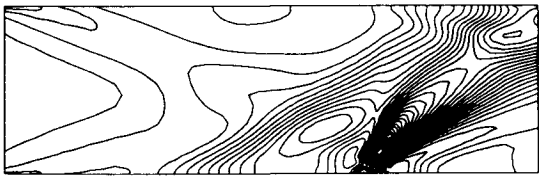

Fig. 2 Static pressure contours of the transverse He injection case.

The final form of the Jacobian A is given as

$$A = \begin{bmatrix} 0 & 1 & 0 & 0 & 0 & 0 & \cdots & 0 \\ (\tilde{\gamma}-1)\left(\frac{q^2}{2}-h^\circ_{f_{N_s}}\right)-u^2 & (3-\tilde{\gamma})u & -(\tilde{\gamma}-1)v & (\tilde{\gamma}-1) & -(\tilde{\gamma}-1)\Delta h^\circ_{f_1} & -(\tilde{\gamma}-1)\Delta h^\circ_{f_2} & \cdots & -(\tilde{\gamma}-1)\Delta h^\circ_{f_{N_s-1}} \\ -uv & v & u & 0 & 0 & 0 & \cdots & 0 \\ \frac{-u}{\rho}(\rho e+p)+(\tilde{\gamma}-1)u\left(\frac{q^2}{2}-h^\circ_{f_{N_s}}\right) & \frac{1}{\rho}(\rho e+p)-(\tilde{\gamma}-1)u^2 & -(\tilde{\gamma}-1)uv & \tilde{\gamma}u & -(\tilde{\gamma}-1)u\Delta h^\circ_{f_1} & -(\tilde{\gamma}-1)u\Delta h^\circ_{f_2} & \cdots & -(\tilde{\gamma}-1)u\Delta h^\circ_{f_{N_s-1}} \\ -uY_1 & Y_1 & 0 & 0 & u & 0 & \cdots & \\ -uY_2 & Y_2 & 0 & 0 & 0 & u & 0\cdots & 0 \\ \vdots & \vdots & \vdots & \vdots & \vdots & \vdots & & \\ -uY_{N_s-1} & Y_{N_s-1} & 0 & 0 & 0 & 0 & 0\cdots & u \end{bmatrix} \tag{22}$$

where $q^2 = u^2 + v^2$. The form of B is similar to that of A.

Equation (18) can now be rewritten in the following form:

$$\left[\mathrm{DIAG}_{i,j} - \frac{A^+_{i-1,j}}{\Delta x} - \frac{B^+_{i,j-1}}{\Delta y}\right]\left[\left(\frac{\nu_A}{\Delta x}+\frac{\nu_B}{\Delta y}\right)I + \frac{A^-_{i+1,j}}{\Delta x} + \frac{B^-_{i,j+1}}{\Delta y}\right]\delta Q = -\left(\frac{\nu_A}{\Delta x}+\frac{\nu_B}{\Delta y}\right)[D_x(F-F_v)+D_y(G-G_v)-S] \tag{23}$$

where

$$\mathrm{DIAG}_{i,j} = \left[\left(\frac{\nu_A}{\Delta x}+\frac{\nu_B}{\Delta y}\right)I - H\right]_{i,j}$$

are the $(N_s + 3) \times (N_s + 3)$ blocks in the diagonal of the matrix operator. These diagonal blocks are of the following form:

$$\mathrm{DIAG} = \begin{bmatrix} (\nu_A+\nu_B) & 0 & 0 & 0 & 0 & \cdots & 0 \\ 0 & (\nu_A+\nu_B) & 0 & 0 & 0 & \cdots & 0 \\ 0 & 0 & (\nu_A+\nu_B) & 0 & 0 & \cdots & 0 \\ 0 & 0 & 0 & (\nu_A+\nu_B) & 0 & \cdots & 0 \\ -\frac{\partial S_5}{\partial \rho} & -\frac{\partial S_5}{\partial \rho u} & -\frac{\partial S_5}{\partial \rho v} & -\frac{\partial S_5}{\partial \rho e} & -\frac{\partial S_5}{\partial \rho Y_1}+(\nu_A+\nu_B) & \cdots & -\frac{\partial S_5}{\partial \rho Y_{N_s-1}} \\ \vdots & \vdots & & & & & \\ -\frac{\partial S_{N_s+3}}{\partial \rho} & -\frac{\partial S_{N_s+3}}{\partial \rho u} & \cdots & \cdots & \cdots & \cdots & -\frac{\partial S_{N_s+3}}{\partial \rho Y_{N_s-1}}+(\nu_A+\nu_B) \end{bmatrix} \tag{24}$$

In Eq. (24), $\partial S_i/\partial \rho = 0$ (since ρ_{Yi} are solved as independent variables), and $\partial S_i/\partial(\rho u)$ and $\partial S_i/\partial(\rho v)$ are taken as zero because they are usually small, although they can be evaluated via the chain rule, e.g.,

$$\frac{\partial S_i}{\partial \rho u} = \left(\frac{\partial S_i}{\partial T}\right)_{\rho Y_i}\left(\frac{\partial T}{\partial \hat{e}}\right)_{\rho,\rho Y_i}\left(\frac{\partial \hat{e}}{\partial \rho u}\right)_{\rho,\rho v,\rho e,\rho Y_i} \tag{25}$$

where T denotes temperature,

$$\hat{e} = e - \frac{u^2+v^2}{2} = h^\circ_{f_m} + \int_{T_{\mathrm{Ref}}}^{T} C_{v_m}\,\mathrm{d}T$$

and

$$C_{v_m} = \sum_{i=1}^{N_s} Y_i C_{v_i}$$

The terms of $\partial S_i/\partial(\rho e)$ in Eq. (24) are evaluated using a chain-rule formula similar to Eq. (25). The $\partial S_i/\partial(\rho Y_j)$ terms can be easily calculated from the law of mass action.[12]

It is interesting to note that, for nonreacting flows [$S = 0$ and $H = 0$ in Eq. (23)], the present numerical method eliminates the need for banded block matrix inversions without using a diagonalization procedure. In fact, with a forward diagonal sweep for the inversion of the first operator and a backward diagonal sweep for the inversion of the second operator, only scalar diagonal inversions are needed to solve Eq. (23) for nonreacting flow problems.

For reacting flows, because of the presence of the chemical source Jacobian H, the first operator on the left-hand side of Eq. (23) now requires block diagonal matrix inversions. Because, however, in the present formulation, the flow equations (continuity, momentum, and energy equations) have no source terms, the first four rows of the diagonal block (DIAG) of this operator have nonzero terms only in the diagonal. As a result, the first operator of Eq. (23) can be inverted in essentially two separate steps: the scalar diagonal matrix inversion for the flow equations and the block diagonal matrix inversion for the species equations. In contrast, most other implicit schemes require block banded (tridiagonal or pentadiagonal) matrix inversions for both operators for either the reacting or nonreacting flows. Here, two advantages in efficiency are obtained by the LU-SSOR scheme over other implicit schemes: 1) The block size is smaller in the LU-SSOR

scheme. Because the operational count is proportional to N^3 for inverting an N × N matrix, the saving in CPU time can be significant; 2) the operational count for inverting a block diagonal matrix is only a fraction of that for inverting a block banded matrix.

Another important efficiency advantage of the LU-SSOR scheme is the vectorizability of its implicit operators. For example, the inversion of the two LHS operators of Eq. (23) can be fully vectorized if the solution sweeps are taken along the diagonal directions (the directions in which the value i and j increase or decrease). It is noted that the vectorizability is unique to the LU scheme and, to the authors' knowledge, no other implicit scheme can have the LHS operators fully vectorized. The vectorizability of the LHS operators is particularly significant for reacting flow calculations because the most time-consuming operation of inverting the chemical source Jacobian matrix can then be executed simultaneously for a large number of points on the same vector plane, resulting in large savings in CPU time.

Boundary and Initial Conditions

For the problems to be considered here, the inflows are always supersonic, so that the upstream boundary conditions are provided by specifying the velocities, static pressure and temperature, and species mass fractions. For the supersonic outflow, the dependent variables are extrapolated from the interior. At the outflow plane, for grid points inside the wall boundary layers where the flow is subsonic, however, static pressure is specified and density is calculated using the ideal gas law. Along the solid wall, no-slip boundary conditions are specified. The wall is assumed to be adiabatic. The normal derivatives of pressure and species concentrations are also assumed to be zero. The injector is assumed to be choked (because of the high injection pressure), and thus all the dependent variables are fixed at their initial values at the injection slot. Along a plane of symmetry, the normal derivatives of all the dependent variables are zero, except for the v velocity, where $v = 0$ is specified.

The governing equations are initialized by setting all the dependent variables throughout the domain to the inflow conditions.

Results and Discussion

One of the main purposes of this paper is to study the mixing and chemical reaction of the transversely injected hydrogen in a supersonic airstream. This flow configuration is of particular interest to scramjet engine design because transverse injection increases the fuel residence time in the combustor and the resulting flow recirculation can help to stabilize the flame. Because this paper is the first application of the LU-SSOR scheme to combustion problems, the ability of the method to compute complex reacting flows is assessed by first computing two simpler flows where either experimental data or previous numerical results are available for comparison. These two are 1) the transverse injection of helium into a supersonic airstream and 2) the combustion of premixed H_2-air supersonic flow in a ramped duct. For all the calculations presented in the paper, the grids are stretched to have finer resolutions in regions of sharp gradients.

Code Assessment

An experiment was conducted by G. O. Kraemer and R. C. Rogers to study details of the flowfield near a slot sonically injecting helium transversely into a ducted supersonic airstream. Results of this experiment were reported by Weidner and Drummond[19] along with their numerical predictions. The experimental apparatus and the inflow conditions are shown in Fig. 1. This test case involves no chemical reactions. Three species, i.e., oxygen, nitrogen, and helium, are included in the calculations.

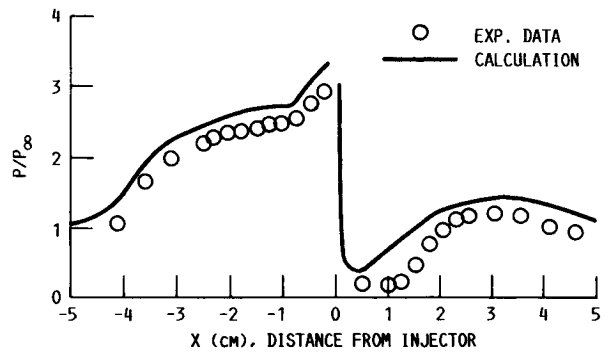

Fig. 3 Static wall pressure of the transverse He injection case.

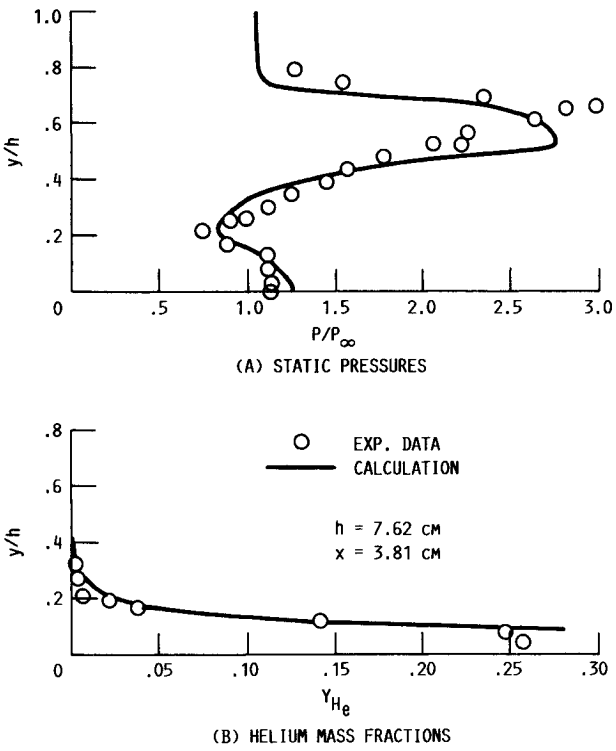

Fig. 4 Comparison of experimental and computed static pressures and helium mass fractions.

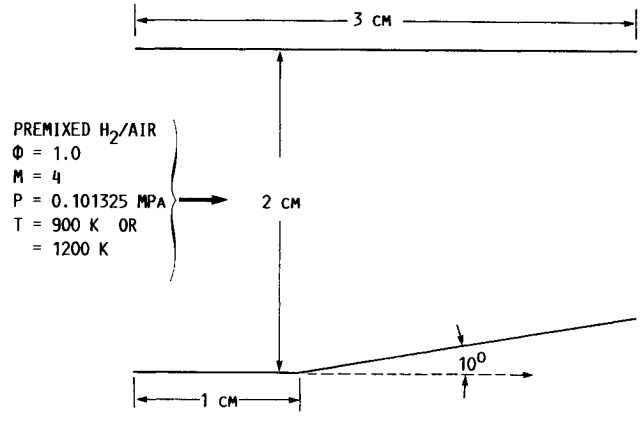

Fig. 5 Geometry and inflow conditions for the premixed H_2/air reacting flows.

Results are given in Figs. 2–4. Figure 2 shows the static pressure contours. The helium jet partially blocks the cross-flow, resulting in a bow shock and strong pressure gradients around the injector. The jet accelerates immediately after injection because of the high injector pressure and then forms several very strong jet shocks further downstream from the injection slot. Figure 3 presents a comparison of the calculated and experimental results for lower wall pressures upstream and downstream of the injection slot, which is located at $x = 0$. The calculations slightly overestimate the peak pressure as well as the distance upstream from the slot injector where the pressure begins to rise. The pressure levels immediately downstream of the injector are also somewhat overpredicted. The cross-stream static pressures and helium mass fractions at 3.81 cm downstream of the injector slot are shown in Fig. 4. The peak pressure caused by the bow shock and the jet shocks is slightly underpredicted. Overall, the agreement between the calculated results and the data is quite good. Considering the very complex flowfield associated with the transverse injection, the performance of the present numerical method is very encouraging.

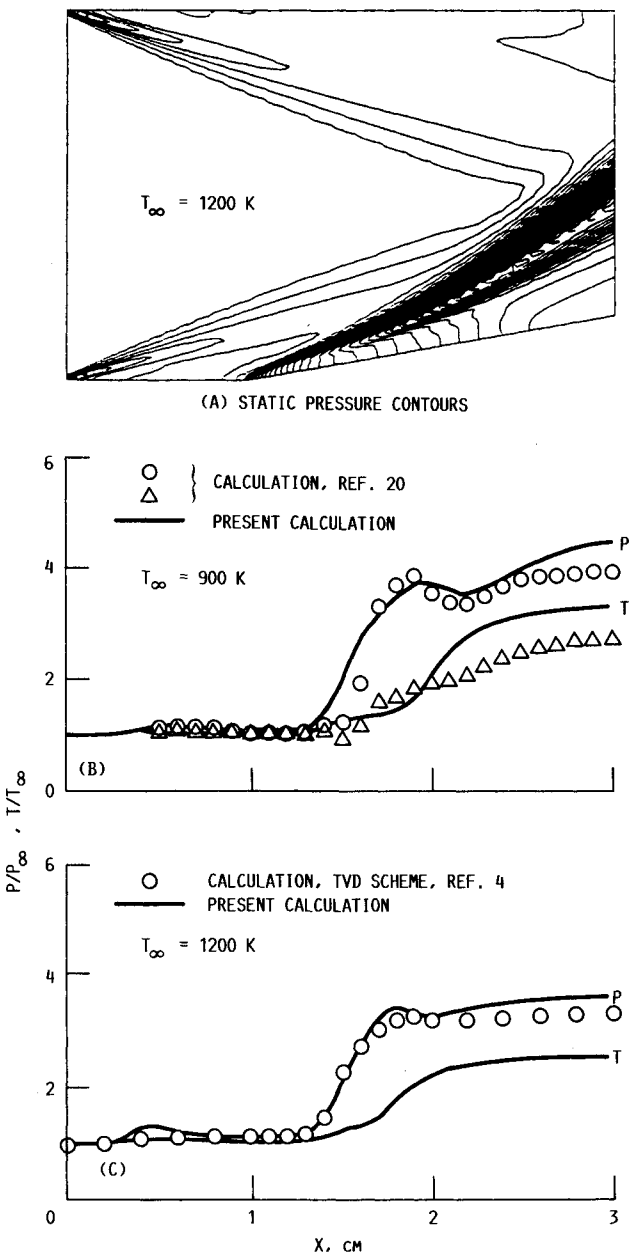

Fig. 6 Static pressure contours, pressure, and temperature along $y = 0.13$ cm.

The next case considered for code assessment is the combustion of a premixed hydrogen-air supersonic flow in a ramped duct. The same flows have been computed by a number of CFD research groups,[3,4,20] and the results of the present method are compared here with those of previous studies.

The geometry and inflow conditions of the two test cases (T_∞ = 900 K and 1200 K) are illustrated in Fig. 5. The inflow is at temperatures below the ignition threshold. The viscous layer along the walls and the shock wave induced by the ramp increase the temperature to a value at which significant reactions occur. The pressure contours for the case of T_0 = 1200 K are shown in Fig. 6a. The leading-edge shocks and the ramp shock are clearly seen. A continual increase of pressure behind the ramp shock resulting from heat released during combustion can also be observed, and this pressure increase in turn causes the ramp shock to bend upward. Comparisons of static pressure and temperature between the present calculations and the results of Refs. 4 and 20 are given in Figs. 6b and c. The results are obtained along the y station located 0.13 cm from the lower wall. It can be seen that the agreement is reasonably good. The present calculation shows higher temperature and pressure behind the ramp shock than indicated by the result of Ref. 20. This is attributed to the different chemical models used in the two studies. As discussed earlier, the reaction time of the 14-step H_2-air chemistry model used in the present study is shorter than the 2-step global model used in Ref. 20 and, as a result, the present model predicts faster and more complete chemical reactions with greater rises in temperature and pressure behind the shock. Both the present results and the results

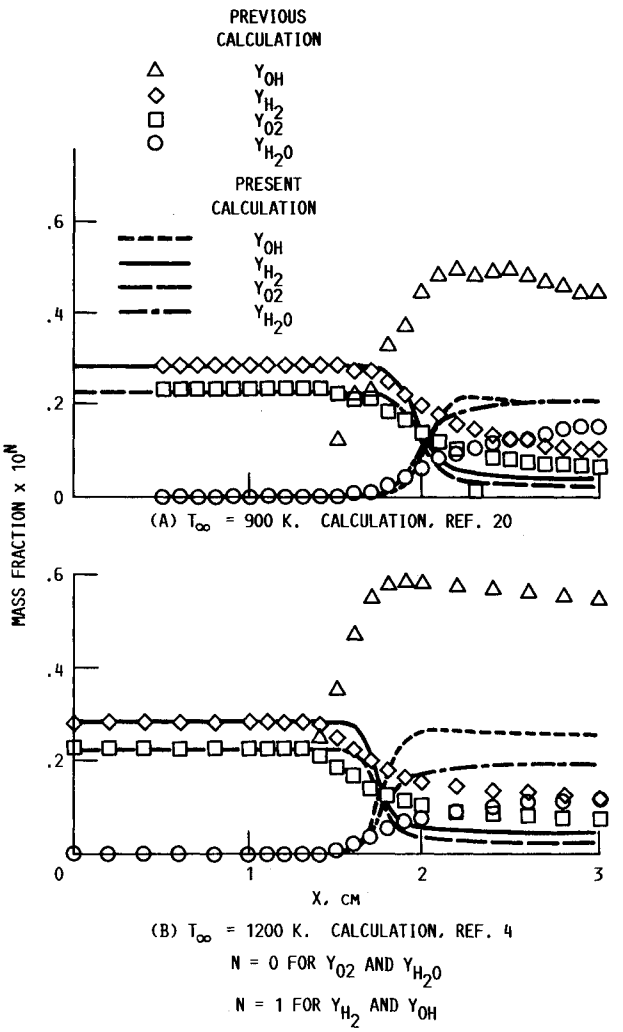

Fig. 7 Comparison of species mass fractions between present and previous numerical predictions.

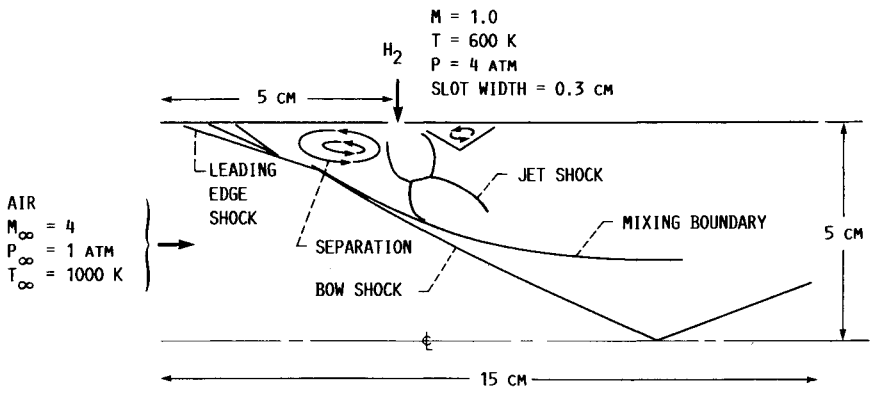

Fig. 8 Geometry and inflow conditions of the transverse hydrogen injection case.

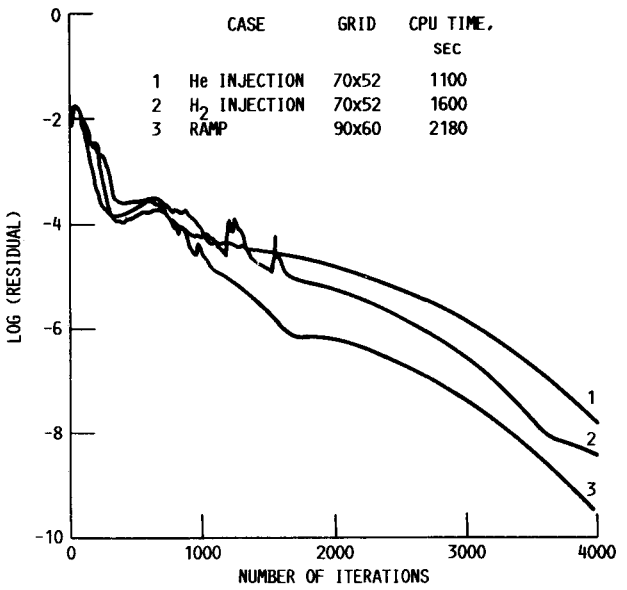

Fig. 9 Convergence history of nondimensionalized L_2 density residual.

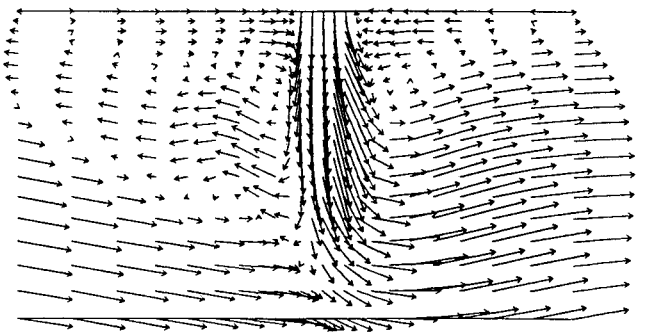

Fig. 10 Velocity vectors around the injector for the H_2-injection case.

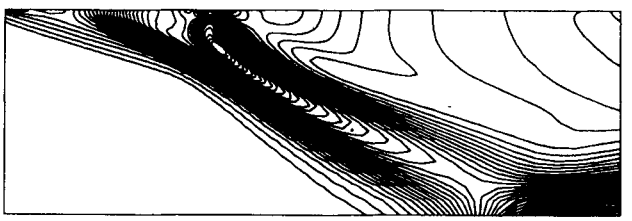

Fig. 11 Static pressure contours for the H_2-injection case.

of Ref. 20 show some oscillations in pressure immediately behind the ramp shock. This is caused by the artificial dissipation models to augment the central-differencing scheme used in the studies. The TVD scheme used in Ref. 4 (Fig. 6c) is seen to give a smoother pressure jump across the shock. Yoon and Kwak[16] also discuss a new flux difference split TVD dissipation model, which recovers a third-order-accurate upwind scheme and which is expected to yield better prediction across the shock.

The distributions of species mass fractions are compared next in Fig. 7. The present results show larger H_2O and smaller OH concentrations behind the shock than those of Refs. 4 and 20, indicating faster and more complete reactions predicted by the 14-step chemistry model. Again, this phenomenon is attributed to the difference in chemistry models used in these studies.

Mixing and Combustion of H_2 Jet in a Supersonic Airstream

To demonstrate further the capability of the present code, the mixing and combustion of a sonic transverse hydrogen jet injected from a slot into a Mach 4 airstream in a two-dimensional duct are computed. The duct geometry, inflow conditions, and main features of the flow structure are illustrated in Fig. 8. The inflow conditions produce a global equivalence ratio of 0.71 (hydrogen/air mass ratio = 0.02). The convergence histories of the numerical calculations for this case and the two cases discussed earlier are shown in Fig. 9. This figure also illustrates the grid density and CPU time (on a CRAY-XMP computer) for each case. Considering that relatively complicated chemistry and thermodynamic and transport property models are used in these calculations, the convergence efficiency shown in Fig. 8 is certainly encouraging.

The velocity vectors around the injector slot are illustrated in Fig. 10. For clarity of presentation, only the velocity vector for every other grid point is shown. A large recirculation zone upstream of the injector can be clearly identified. The flow separation is caused by the adverse pressure gradient produced by the hydrogen jet and the shock boundary-layer interactions. There is also a smaller region of separation downstream of the injector caused by the blockage of flow by the hydrogen jet. In scramjet engines, the two recirculation regions provide longer fuel residence times as well as better mixing of fuel, air, and hot combustion gas, resulting in better flameholding capabilities for the combustor. The static pressure contours are shown in Fig. 11. The injected high-pressure fluid expands rapidly and yields large pressure gradients along its path. Both this figure and the schematic flowfield shown in Fig. 8 indicate that the hydrogen jet partially blocks the axial flow and generates a strong bow shock just ahead of the injector. The hydrogen jet accelerates to supersonic speed immediately after injection and then soon decelerates by jet shocks. The incidence and reflection (by the uprunning bow shock from the bottom half of the duct) of the bow shock to and from the symmetric

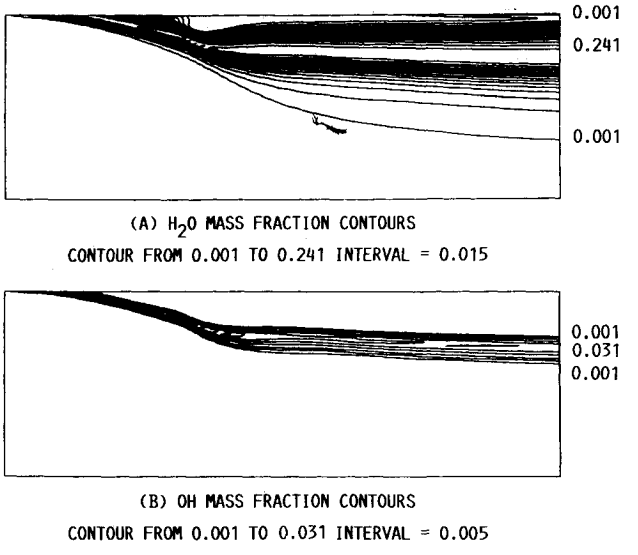

Fig. 12 H_2O and OH mass fraction contours for the H_2-injection case.

plane of the duct can also be seen in Fig. 11. The contour maps of the mass fractions of two major combustion products (i.e., H_2O and OH) are presented in Fig. 12. The large mass fractions of H_2O and OH found in the recirculation zone in front of the injector indicate that transverse injection of fuel provides good flameholding capability for the simulated transverse jet flow.

Concluding Remarks

A computer code (RPLUS) for analyzing two-dimensional chemically reacting flowfields has been developed. It employs the LU-SSOR finite-volume scheme, which solves the Navier-Stokes and species transport equations in a fully implicit and coupled manner. Its validity is demonstrated by comparisons of the present calculations with experimental data and previous numerical results. The code has been used to calculate the flowfield in a two-dimensional duct in which the hydrogen is transversely injected into a supersonic airstream. The present results show that the new code has the potential to handle the complex flowfield associated with the fuel injection, mixing, and chemical reactions in a scramjet combustor. The new code has also been shown to be very efficient and robust for the flows considered in the present study.

Interactions between the turbulence and chemical reactions are not accounted for in the present study. The interaction effects are important in most ramjet/scramjet combustor flows, especially for simulating ignition, flameholding stability, and heat release rate, and should be considered in future code improvement efforts.

References

[1]Bussing, T. R. A. and Murman, E. M., "A Finite Volume for the Calculation of Compressible Chemically Reacting Flows," AIAA Paper 85-0331, Jan. 1986.

[2]Eklund, D. R., Hassan, H. A., and Drummond, J. P., "The Efficient Calculation of Chemically Reacting Flow," AIAA Paper 86-0563, Jan. 1986.

[3]Uenishi, K., Rogers, R. C., and Northam, G. B., "Three-Dimensional Computations of Transverse Hydrogen Jet Combustion in a Supersonic Airstream," AIAA Paper 87-0089, Jan. 1987.

[4]Shinn, J. L., Yee, H. C., and Uenishi. K., "Extension of a Semi-Implicit Shock-Capturing Algorithm for Three-Dimensional Fully Coupled Chemical Reacting Flows in Generalized Coordinates," AIAA Paper 87-1577, 1987.

[5]Beam, R. M. and Warming, R. F., "An Implicit Finite-Difference Algorithm for Hyperbolic Systems in Conservation-Law Form," *Journal of Computational Physics,* Vol. 22, Sept. 1976, pp. 87–110.

[6]Yoon, S. and Jameson, A., "An LU-SSOR Scheme for the Euler and Navier-Stokes Equations," AIAA Paper 87-600, Jan. 1987.

[7]Jameson, A. and Yoon, S., "Lower-Upper Implicit Schemes with Multiple Grids for the Euler Equations," *AIAA Journal,* Vol. 25, July 1987, pp. 929–935.

[8]Westbrook, C. K., "Hydrogen Oxidation Kinetics in Gaseous Detonations," *Combustion Science and Technology,* Vol. 29, No. 1–2, Jan. 1982, pp. 67–81.

[9]Hitch, B. D., Laxter, W. R., Senser, D. W., and Sojka, P. E., "On the Selection of H_2/Air Kinetic Mechanisms for Use in Supersonic Combustor Modeling," Presented at the Spring 1986 Technical Meeting of the Central States Section of the Combustion Institute. Cleveland, OH, May 1986.

[10]Baldwin, B. and Lomax, H., "Thin Layer Approximation and Algebraic Model for Separated Turbulent Flows," AIAA Paper 78-257, Jan. 1978.

[11]Shuen, J. S., "Effects of Droplet Interactions on Droplet Transport at Intermediate Reynolds Numbers," AIAA Paper 87-0137, Jan. 1987.

[12]Williams, F. A., *Combustion Theory,* 2nd Ed., Benjamin/Cummings Publishing, Menlo Park, CA, 1985, pp. 631–645.

[13]McBride, B. J., Private communication, NASA Lewis Research Center, Cleveland, OH, April 1987.

[14]Reid, R. C., Prausnitz, J. M., and Sherwood, T. K., *The Properties of Gases and Liquids,* 3rd Ed., McGraw-Hill, New York, 1977.

[15]Rogers, R. C. and Chinitz, W., "Using a Global Hydrogen-Air Combustion Model in Turbulence Reacting Flow Calculations," *AIAA Journal,* Vol. 21, April 1983, pp. 586–592.

[16]Yoon, S. and Kwak, D., "Artificial Dissipation Models for Hypersonic Internal Flows," AIAA Paper 88-3277, July 1988.

[17]Shuen, J. S., Liou, M. S., and Van Leer, B., "Inviscid Flux-Splitting Algorithms for Real Gases with Nonequilibrium Chemistry," Paper submitted to Journal of Computational Physics.

[18]Colella, P. and Glaz, H. M., "Efficient Solution Algorithms for the Riemann Problem for Real Gases," *Journal of Computational Physics,* Vol. 59, June 1985, pp. 264–289.

[19]Weidner, E. H. and Drummond, J. P., "Numerical Study of Staged Fuel Injection for Supersonic Combustion," *AIAA Journal,* Vol. 20, Oct. 1982, pp. 1426–1431.

[20]Chitsomboon, T., Kumar, A., and Tiwari, S. N., "Numerical Study of Finite-Rate Supersonic Combustion Using Parabolized Equations," AIAA Paper 87-0088, Jan. 1987.